Video Article

Fabrication of a Biomimetic Nano-Matrix with Janus Base Nanotubes and Fibronectin for Stem Cell Adhesion

Libo Zhou[1], Anne Yau[1], Wuxia Zhang[1], Yupeng Chen[1]

[1]Department of Biomedical Engineering, University of Connecticut

Correspondence to: Yupeng Chen at yupeng.chen@uconn.edu

URL: https://www.jove.com/video/61317
DOI: doi:10.3791/61317

Keywords: Bioengineering, Issue 159, nano-matrix, self-assembled, Janus base nanotubes, fibronectin, mesenchymal stem cells, adhesion

Date Published: 5/10/2020

Citation: Zhou, L., Yau, A., Zhang, W., Chen, Y. Fabrication of a Biomimetic Nano-Matrix with Janus Base Nanotubes and Fibronectin for Stem Cell Adhesion. *J. Vis. Exp.* (159), e61317, doi:10.3791/61317 (2020).

Abstract

A biomimetic NM was developed to serve as a tissue-engineering biological scaffold, which can enhance stem cell anchorage. The biomimetic NM is formed from JBNTs and FN through self-assembly in an aqueous solution. JBNTs measure 200-300 µm in length with inner hydrophobic hollow channels and outer hydrophilic surfaces. JBNTs are positively charged and FNs are negatively charged. Therefore, when injected into a neutral aqueous solution, they are bonded together via noncovalent bonding to form the NM bundles. The self-assembly process is completed within a few seconds without any chemical initiators, heat source, or UV light. When the pH of the NM solution is lower than the isoelectric point of FNs (pI 5.5-6.0), the NM bundles will self-release due to the presence of positively charged FN.

NM is known to mimic the extracellular matrix (ECM) morphologically and hence, can be used as an injectable scaffold, which provides an excellent platform to enhance hMSC adhesion. Cell density analysis and fluorescence imaging experiments indicated that the NMs significantly increased the anchorage of hMSCs compared to the negative control.

Introduction

Human mesenchymal stem cells (hMSCs) have shown the potential for self-renewal and self-differentiation along different mesenchymal lineages, which helps in the regeneration and maintenance of tissues[1]. Based on the differentiation potential, hMSCs are considered as candidates for mesenchymal tissue injuries and hematopoietic disorder therapy[2]. hMSCs have shown the ability to promote wound healing by increasing tissue repair, angiogenesis, and reducing inflammation[3]. However, without biochemical or biomaterials assistance, the efficiency for the hMSCs to reach a target tissue and function at the desired location is low[4]. Although various engineered scaffolds have been utilized to attract hMSCs to adhere onto the lesions, some sites such as growth plate fracture, in the middle of a long bone, are not easily accessible by the conventional pre-fabricated scaffolds, which may not fit perfectly into an irregularly shaped injured site.

Here, we have developed a biomimetic nanomaterial that can self-assemble in situ and be injected to a hard to reach target area. The injectable bio-scaffold NM is composed of Janus base nanotubes (JBNTs) and fibronectin (FN). JBNTs, also known as the Rosette Nanotubes (RNTs), are derived from DNA base pairs, specifically thymine and adenine, here[5,6,7]. As seen in **Figure 1**, the nanotubes are formed when six molecules of the derived DNA base pairs self-assemble via hydrogen bonds to form a plane[6]. Six molecules are then stacked onto each other in a plane via a strong pi-stacking interaction[7], which can be up to 200-300 µm in length. The JBNTs are designed to morphologically mimic collagen fibers so that FN will react with them.

FN is a high molecular weight adhesive glycoprotein, which can be found in the extracellular matrix (ECM)[9]. These can mediate the attachment of stem cells to other components of the ECM, particularly collagen[10]. We designed JBNTs to morphologically mimic collagen fibers so FN can react with them to form NM in a few seconds via noncovalent bonding. Therefore, NM is a promising bio-scaffold to be injected into a bone fracture site that could not be accessible by the conventionally fabricated scaffolds. Here, the injectable NM presents an excellent ability to enhance hMSC anchorage in vitro, exhibiting their potential to serve as a scaffold for tissue regeneration.

Protocol

1. Synthesis of JBNTs

NOTE: JBNT monomer was prepared as published previously[11].

1. Synthesis of compound A1
    1. Prepare a solution containing 8.50 g of 2-cyanoacetic acid and 9.80 g of ethylcarbamate in 25 mL of toluene and 2.5 mL of N, N-dimethylformamide. Add 4.90 mL of phosphoryl chloride dropwise. Then heat the mixture to 70 °C and keep stirring for 1.5 h.
    2. Cool the reaction mixture to room temperature and pour in 100 g of ice water. Extract the aqueous layer with ethyl acetate (3 x 250 mL), and wash with 100 mL of brine. Dry the organic layer over anhydrous sodium sulfate, filter and evaporate volatiles under vacuum to get a pale-yellow solid.

3. Subject the yellow solid to silica gel flash column chromatography (3% methanol/dichloromethane) to yield 15.61 g of compound A1 as a white powder.

2. Synthesis of compound A2
    1. Mix 3.12 g of compound A1 and 2.75 g of potassium carbonate in 50 mL of N, N-dimethylformamide. Stir at room temperature for 2 h.
    2. Add 2.6 mL of carbon disulfide to the reaction suspension. Keep stirring for 4 h.
    3. Add absolute ethanol to the reaction mixture at 0 °C. Filter the yellow precipitate out and wash with diethyl ether. Dry under vacuum overnight to yield 6.18 g of compound A2 as pale-yellow solid.

3. Synthesis of compound A3
    1. Add 2.7 mL of methyl iodide in 15 mL of acetonitrile. Also, separately prepare a solution of compound A2 by adding 6.18 g of A2 to 80 mL of water/acetonitrile (7:3 ratio). Mix both the solutions and stir at room temperature for 30 min.
    2. Heat the reaction mixture to 95 °C and keep stirring for 3 h.
    3. Cool the reaction mixture to room temperature, and then evaporate the volatiles under vacuum.
    4. Extract the residue 3x with 100 mL of ethyl acetate and wash with brine. Dry the organic layer over anhydrous sodium sulfate, filter and evaporate the volatiles under vacuum to obtain a yellow solid.
    5. Subject the yellow solid to silica gel flash column chromatography (30% ethyl acetate/hexanes) to yield 4.52 g of the compound A3 as a light-yellow solid.

4. Synthesis of compound A4
    1. Prepare allylamine solution by adding 925 µL of allylamine in 20 mL of ethanol. Add this solution dropwise to the solution of compound A3, prepared by adding 3.14 g of A3 in 75 mL of absolute ethanol, over 30 min. Then heat the reaction mixture to reflux for 16 h.
    2. Cool the reaction mixture to room temperature and evaporate the volatiles to give a yellow solid.
    3. Subject the yellow solid to silica gel flash column chromatography (50% ethyl acetate/hexanes to 2% methanol/dichloromethane) to yield 1.80 g of compound A4 as a white crystal.

5. Synthesis of compound A5
    1. Add 2.05 g of guanidinium hydrochloride and 7.8 mL of sodium ethoxide (21 wt% in ethanol) in 14 mL of absolute ethanol. Heat the mixture to 45 °C for 15 min.
    2. Filter off the insoluble material and add the filtrate directly into the solution of compound A4, prepared by adding 2.70 g of A4 in 40 mL absolute ethanol. Heat the reaction mixture to reflux for 16 h.
    3. Filter the precipitate out to obtain 2.65 g of compound A5 as an off-white solid.

6. Synthesis of compound A6
    1. Add 24.9 mL of triethylamine slowly to the slurry mixture obtained by adding 2.11 g of compound A5 and 1.10 g of 4-Dimethylaminopyridine in 120 mL of tetrahydrofuran over 1 min. Stir at room temperature for 2 min.
    2. Add 20.7 mL of di-tert-butyl dicarbonate dropwise to the reaction mixture and keep stirring at room temperature for 40 h.
    3. Add 20 mL of water to quench the reaction. Evaporate the volatiles under vacuum.
    4. Extract the red viscous residue with 500 mL of ethyl acetate. Then, wash it in with 250 mL of water, 75 mL of 10% citric acid, 2x with 200 mL of water, 200 mL of saturated sodium bicarbonate, and 200 mL of brine. Dry the organic layer over anhydrous sodium sulfate, filter and evaporate the volatiles under vacuum to give a red/orange solid.
    5. Subject the solid to silica gel flash column chromatography (0-20% ethyl acetate/hexanes) to yield 3.87 g of compound A6 as a white foam.

7. Synthesis of compound A7
    1. Add N-methylmorpholine N-oxide (50 wt.% in water, 1.64 mL) dropwise to the solution of compound A6 (2.93 g) in acetone/water (8:1, 58.5 mL) and stir at room temperature for 5 min.
    2. Add osmium tetraoxide (4% aqueous solution) dropwise to the mixture over a period of 3 min and keep stirring at room temperature for 24 h.
    3. Quench the reaction with 1.0 M aqueous sodium sulfite until the solution turns colorless. Remove the volatiles under vacuum to result in a white slurry in water. Extract the residue with 350 mL of dichloromethane and then wash with 150 mL of water followed by a wash with 150 mL of brine.
    4. Dry the organic layer over anhydrous sodium sulfate, filter and evaporate the volatiles under vacuum to yield 2.45 g of compound A7 as a white solid.

8. Synthesis of compound A8
    1. Add 760 g of sodium periodide to the mixture of 1.36 g of compound A7 in 35 mL of dichloromethane/water (6:1, 35 mL) and stir at room temperature for 42 h.
    2. Filter the insoluble material off and concentrate the filtrate under vacuum. Extract the resulting residue with 250 mL of dichloromethane, and then wash with 100 mL of water and 100 mL of brine. Dry the organic layer over anhydrous sodium sulfate, filter and evaporate the volatiles under vacuum to give the crude product.
    3. Subject the crude product to silica gel flash column chromatography (5-40% ethyl acetate/hexanes, then 5% methanol/dichloromethane) to yield 1.08 g of compound A8.

9. Synthesis of compound A9
    1. Prepare a solution of 830 mg of compound A8 in 15 mL of 1,2-dichloroethane. Add the solution of dropwise to the mixture of 6-benzyloxycarbonylamino-2-L-amino-hexanoic acid trimethylsilyl ethyl ester (649.5 mg) and N,N-diisopropylethylamine (591 µL) in 24 mL of 1,2-dichloroethane over 3 min and stir at room temperature for 15 min.
    2. Add 360.3 mg of sodium triacetoxyborohydride to the solution and keep stirring at room temperature for 24 h.

3. Quench the reaction mixture with 6 mL of water. Extract the reaction mixture 3x with 200 mL of dichloromethane and wash with 200 mL of 10% citric acid in water, 2x with 200 mL of water, 200 mL of saturated sodium bicarbonate, and 200 mL of brine in that order. Dry the organic layer over anhydrous sodium sulfate, filter and evaporate the volatiles under vacuum to obtain the crude product.
4. Subject the crude product to silica gel flash column chromatography (5-30% ethyl acetate/hexanes) to yield 885 mg compound A9.

10. Synthesis of JBNT monomer
    1. Dissolve 0.54 g of compound A9 (0.54 g) in 10 mL of 94% trifluoroacetic acid/thioanisole solution and stir at room temperature for 72 h.
    2. Add diethyl ether (80 mL) to the reaction mixture and centrifuge the precipitate down. Pour the clear trifluoroacetic acid containing supernatant out and wash the white precipitate with diethyl ether and methanol to yield 168.6 mg crude JBNT monomer (**Supplemental File 1**).
    3. Purify the crude JBNT monomer by a high-performance liquid chromatography (HPLC) with a reverse phase column. The isolation program is listed below: Solvent A: 100% water; solvent B: 100% acetonitrile; solvent C: pH=1 HCl water solution; flow rate: 3 mL/min (see **Table 1**).
    4. Collect the largest peak at about 7.2 min.

2. Fabrication for JBNT/FN

1. Add 80 µL of 1 mg/mL JBNT aqueous solution to 40 µL of 1 mg/mL FN aqueous solution and pipette several times.
2. Check for the presence of white solid suspension after pipetting for about 10 s.
   NOTE: A video was shot to capture the self-assembly process of NM (**Supplemental File 2**).

3. Observation of lyophilized specimens

NOTE: This step is performed to show the scaffold structure of NM made from JBNTs and FN.

1. Prepare FN, JBNT and FN/JBNT NM solutions for lyophilized materials observation. Dilute 10 µL of 100 µg/mL of FN with 40 µL of distilled water to make a 20 µg/mL solution of FN.
2. Prepare 100 mg/mL solution of JBNTs by diluting 5 µL of 1 mg/mL JBNTs in 45 µL of DI water.
3. Mix 10 µL of 100 µg/mL FN and 5 µL of 1 mg/mL of JBNTs in 35 µL of DI water to form the NM solution.
4. Coat three wells of 96-well clear round bottom microplates with the FN, JBNT solution and NM solution, respectively. Each well receives 50 µL of the solution.
5. Perform lyophilization, as described below, to visualize the scaffold structure of the NM.
    1. Freeze the plate at -80 °C overnight.
    2. Turn on the lyophilized instrument and vacuum pump.
    3. Press the **cool down** button to reduce the temperature of the system to -50 °C.
    4. Put the frozen plate into the lyophilized instrument and close all openings of the instruments.
    5. Click the **start** button to reduce the system pressure to 0.9 mbar.
    6. After 4 h, press the **aerate** button and open the valve to increase the system pressure to the atmospheric pressure.
    7. Take the plate out of the lyophilized instrument.
    8. Use a microscope to observe the FN, JBNTs and the resulting self-assembled NM. Take several photographs with a camera for the materials.

4. Absorption spectra measurement

NOTE: Use the change of spectra for FN and JBNTs to present the self-assembled JBNT/FN NM[12].

1. Mix 30 µL of 100 µg/mL FN with 15 µL of distilled water and 5 µL of 1 mg/mL JBNTs to prepare the JBNT/FN NM solution. White solid suspension can be seen after pipetting the solution several times.
   NOTE: The final concentrations of JBNTs and FN in the solution are 100 µg/mL and 60 µg/mL, respectively. JBNTs and FN solutions at the same concentration to the one used in the NM solution were also prepared as control solutions.
2. Dilute 5 µL of 1 mg/mL of JBNTs with 45 µL of distilled water to prepare JBNT control solution.
3. Dilute 30 µL of 100 µg/mL FN with 20 µL of distilled water to prepare FN control solution.
4. Measure the UV-vis absorption spectra of FN, JBNT and JBNT/FN NM solutions with the spectrophotometer (see **Table of Materials**) to characterize the assembly of NM.
    1. Click the **UV-Vis** button. Clean the test surface of the spectrophotometer and drop 2 µL of distilled water on it. Measure it as blank from 190-850 nm.
    2. Clean the test surface of the spectrophotometer and drop 2 µL of FN solution on it. Measure the UV-Vis absorption spectra of FN solution from 190 nm to 850 nm.
    3. Clean the test surface of the spectrophotometer and drop 2 µL of JBNT solution on it. Measure the absorption spectra of JBNT solution from 190 nm to 850 nm.
    4. Clean the test surface of the spectrophotometer and drop 2 µL of JBNT/FN NM solution on it. Measure the absorption spectra of JBNT/FN NM solution from 190 nm to 850 nm.

5. Preparation of JBNT/FN NM for transmission electronic microscopy (TEM)

1. Clean several grids before negative staining with a basic plasma cleaner (see **Table of Materials**).
2. Perform the negative staining for the specimens following two different processes.
    1. Drop 3 µL of 1 mg/mL of JBNTs aqueous solution and 3 µL of JBNT/FN NM solution on separated grids and leave it for 2 min. Then rinse each grid with 100 µL of 0.5% uranyl acetate (UA) solution. Drain the excess solution with filter paper and air dry the grids.
    2. Mix 9 µL of JBNT/FN NM solution with 3 µL of 2.0% UA solution and pipette it several times. Pipette the mixed solution on the grids and keep it on the grids for 2 min. Use a filter paper to remove the mixed solution from the grids and dry the grids at room temperature.
3. Finally, characterize the specimen for JBNTs, JBNT/FN NM stained with step 5.2.1, and JBNT/FN NM stained with step 5.2.2 with the TEM.

6. In vitro biological function assay

1. Add 200 µL of negative controls (NC, PBS), JBNTs, FN and the JBNT/FN NM solutions into one well of an 8-well chambered slide, respectively.
2. Freeze dry the 8-well chambered coverglass with the lyophilized instrument to coat materials on the bottom of wells. The protocol for freeze-drying is the same as step 3.5.
3. Then add 10,000 cells/wells hMSCs (Passage 3) into the wells and incubate them for 24 h at 37 °C with 5% CO_2.
4. After incubation, pipette out the cell culture medium from the wells and rinse the culture with 1x PBS solution.
5. Add 100 µL of the fixative solution to each well with cells and leave for 5 min. Rinse cells gently with 1x PBS twice.
6. Dilute 1% Triton-X 100 to 0.1%. Add 100 µL of 0.1% Triton-X 100 to each well with cells and leave for 10 min. Rinse cells gently with 1x PBS twice.
7. Dilute the Rhodamine Phalloidin to 1.65 µM. Add 100 µL of Rhodamine Phalloidin to each well with cells and incubate the chambered coverglass keeping from light at room temperature for 30 min. Rinse cells gently with 1x PBS twice.
8. Capture the cell images with a fluorescent microscope.
9. Count the cell numbers on fluorescent images for each group. Calculate the cell adhesion density by averaging of three random areas in each well.
10. Present all data as average ± standard deviation (SD). Perform statistical analyses using a one-tailed t-test, followed by analysis of variance (ANOVA) with $p<0.05$, which is considered statistically significant.

Representative Results

Our studies discovered that the formation of the NM of JBNTs and FN is fast, which happened in 10 seconds. As shown in **Figure 2**, white floccule was obtained when the JBNT solution was mixed with the FN solution and pipetted several times. The formation process of NM is completely biomimetic. No external stimuli are needed. The process of fabrication is much easier than that of some emerging biomaterials, which is based on ultraviolet light or chemical initiator for crosslinking[13].

We captured and analyzed the camera images of FN, JBNTs, and the NM (**Figure 3**). For the FN group, except for short white spots, no long fibers were observed. The short clusters were the protein agglomerations consisting of FN, which indicates that the scaffold structure cannot be formed with FN alone without JBNTs (**Figure 3A**). As shown in **Figure 3B**, the long and thinner fibers indicate the existence of JBNTs. The width of the white strands of the NM is wider compared to JBNTs, indicating that the JBNTs and FN crosslinked with each other forming NM. The NM fiber can grow up to several centimeters in length (**Figure 3C**).

We obtained the UV-Vis spectra to indicate the assembly between JBNTs and FN. As shown in **Figure 4**, JBNTs exhibits two absorption peaks at 220 nm and 280 nm, respectively. Compared to JBNTs, the JBNT/FN NM has two absorption peaks at the same location with a significantly reduced value, which was from JBNTs but affected by the non-covalent self-assembled JBNTs and FN in between.

TEM was used to characterize the morphology of the JBNTs and NM. As shown in **Figure 5A**, the JBNTs are slender tubes with uniform diameters. Under neutral conditions, JBNTs are positively charged while FN are negatively charged. When mixed, they formed long fibroid NM via charge interactions (**Figure 5B**). When pH is lower than the isoelectric point of the FN (pI of 5.5-6.0), the NM bundles present self-release due to the positively charged FN. As shown in **Figure 5C**, when preserved in a solution with low pH (4.0), the NM was dissembled, and a lot of FN was released from the NM. The FN distributed alongside the nanotube is also a strong evidence that the NM was fabricated by JBNTs and FN[10].

We explored the effect of the JBNT/FN NM on cell adhesion. As shown in **Figure 6**, the cell adhesion density of the NM group showed significant difference (p-value <0.05) value compared to the negative control. The difference may be because the NM are designed to morphologically mimic ECM, which provide a scaffold for cell adhesion[14]. The ECM was composed of collagens and cell adhesive glycoproteins, such as fibronectin[15]. Collagen has been presented with the ability to promote higher adhesion and proliferation of hMSCs[16]. Additionally, fibronectin has been shown to enhance the hMSCs adhesion in the injured site as well[15]. Fluorescence imaging also demonstrated that the hMSCs adherence of the NM group increased significantly compared to the negative control group (**Figure 7**)[15,17].

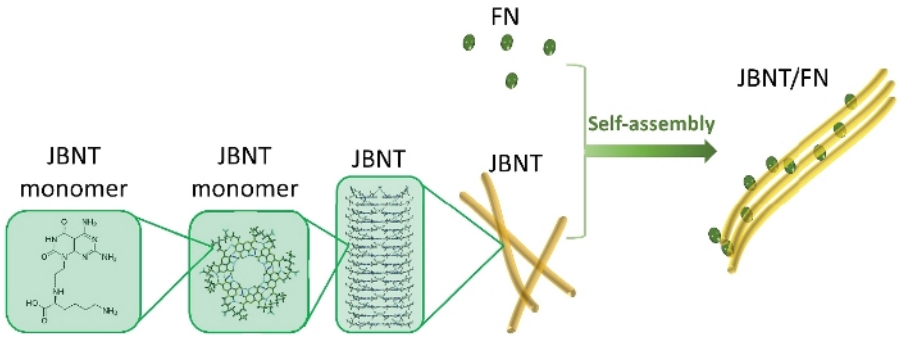

Figure 1: Schematic illustration of the hierarchical self-assembly of JBNTs with a lysine side chain.
This figure is reprinted with permission from the previous publication[12]. Please click here to view a larger version of this figure.

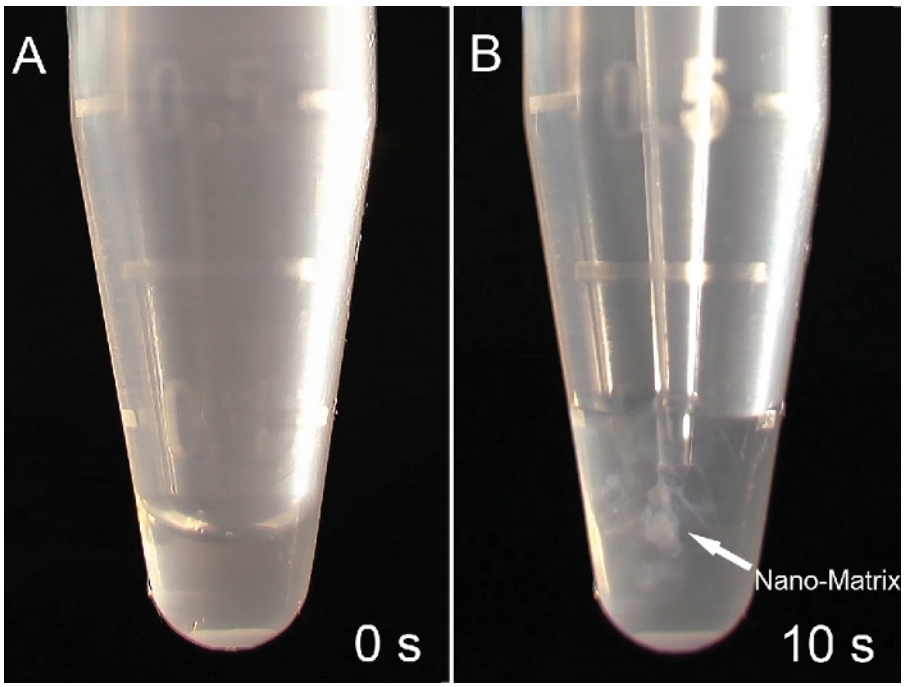

Figure 2: Demonstration for the self-assembled process of the NM.
(**A**) FN solution. (**B**) JBNTs mixed with FN. This figure is reprinted with permission from the previous publication[12]. Please click here to view a larger version of this figure.

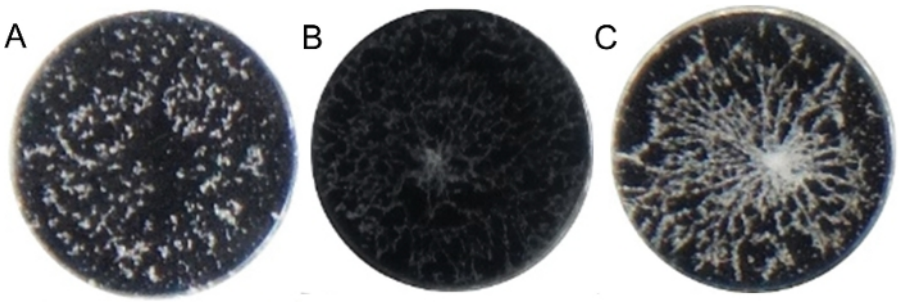

Figure 3: Brightfield photographs.
Brightfield photographs of (**A**) FN (**B**) JBNTs and (**C**) NM formed by JBNTs and FN. Each area has a diameter of 2 cm. This figure is reprinted with permission from the previous publication[12]. Please click here to view a larger version of this figure.

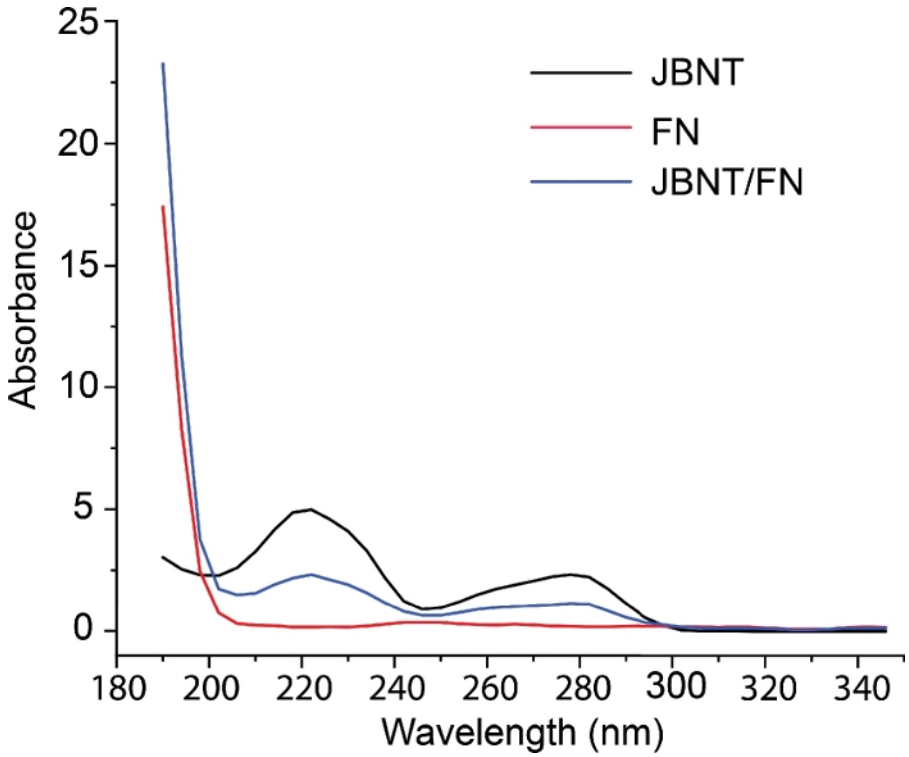

Figure 4: Absorption spectra of FN, JBNTs, and JBNT/FN NM.
This figure is reprinted from the previous publication[12]. Please click here to view a larger version of this figure.

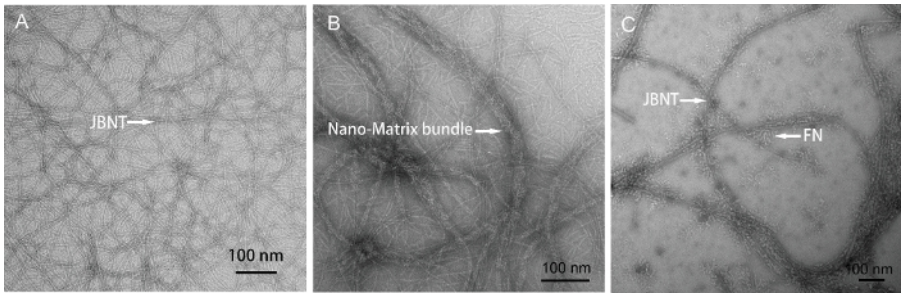

Figure 5: TEM images.
TEM images of (**A**) JBNTs (**B**) JBNT/FN NM, and (**C**) released JBNT/FN NM. This figure is reprinted with permission from the previous publication[12]. Please click here to view a larger version of this figure.

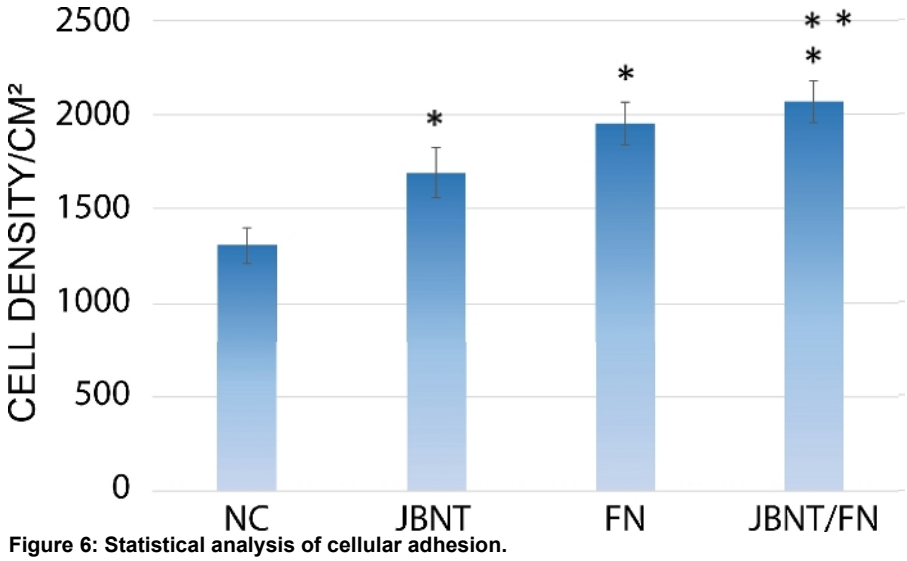

Figure 6: Statistical analysis of cellular adhesion.
Cell adhesion density was recorded in this experiment. *p<0.01 compared to negative controls. **p<0.05 compared to JBNT alone. N=3. This figure is reprinted with permission from the previous publication[12]. Please click here to view a larger version of this figure.

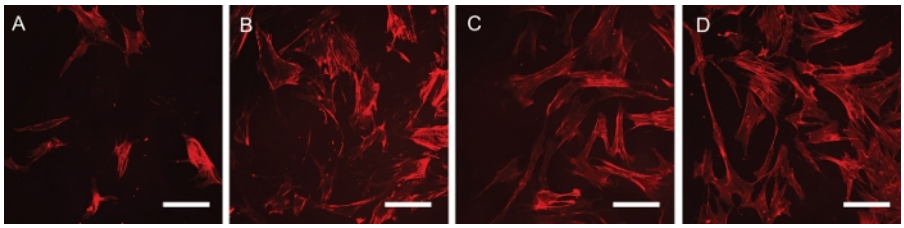

Figure 7: Fluorescence images.
Fluorescence images of (**A**) the hMSCs and (**B**) the hMSC incubated with the JBNTs. (**C**) the hMSC incubated with the FN. (**D**) the hMSC incubated with the JBNT/FN NM. Scale bar: 100 μm. This figure is reprinted with permission from the previous publication[12]. Please click here to view a larger version of this figure.

Time	A%	B%	C%
0.00 min	98	0	2
15.00 min	68	30	2
25.00 min	8	90	2
26.00 min	0	100	0

Table 1: Gradient elution time.

Supplemental File 1: Scheme for the synthesis of JBNT monomer. Please click here to download this figure.

Supplemental File 2: Video for self-assembly of the FN/JBNT NM. Please click here to download this video.

Discussion

In this study, we developed a self-assembled biomimetic NM, which was formed with DNA-inspired JBNTs and FN. When preparing the JBNT solution, the JBNT lyophilized powder should be dissolved into the water instead of PBS because PBS will cause agglomeration of JBNTs, which inhibits their assembly. Moreover, the NM should also be assembled in water if we want to observe the nano-fibril structures of the NM, because the salt in PBS will bundle with NM fibers, which can greatly reduce the resolution of the images.

The NM has shown great potential to serve as a novel tissue engineering scaffold although a lot of efforts have been made to fabricate tissue regenerative scaffolds, which were used to facilitate hMSCs adhesion and differentiation. However, most of these materials are pre-made with a specific shape, such as a 3D printed scaffold[18,19]. As such, they are not easy to be implanted into injured sites that are deep in the joint. However, the NM solution here can be injected as a liquid and then serve as a scaffold for cell adhesion.

One limitation is that the NM is not mechanically strong. Unlike polymers, they are fabricated via self-assembly of noncovalent interactions, so they cannot bear a lot of mechanical loading or tension. On the other hand, the noncovalent structure also presents very good biodegradability and biocompatibility suitable for biological functions[8,20,21].

The injectable NM has shown great potential to provide a target location and a scaffold for MSC homing to enhance bone fracture healing in the body. However, when injected into the injured site, the noncovalent NM may not stay in place for a long time, which may reduce the therapeutic effect. In the future, we will explore to incorporate other materials (such as hydrogels) or to alternate the NM structures to further optimize the properties of the NM scaffold.

Disclosures

Dr. Yupeng Chen is a co-founder of NanoDe Therapeutics, Inc.

Acknowledgments

This work is financially supported by NIH (Grants 1R01AR072027-01, 1R03AR069383-01), NSF Career Award (1653702) and University of Connecticut.

References

1. Yao, W. et al. Improved mobilization of exogenous mesenchymal stem cells to bone for fracture healing and sex difference. *Stem Cells.* **34** (10), 2587-2600 (2016).
2. Salasznyk, R. M., Williams, W. A., Boskey, A., Batorsky, A., Plopper, G. E. Adhesion to vitronectin and collagen I promotes osteogenic differentiation of human mesenchymal stem cells. *Journal of Biomedicine and Biotechnology.* **1** (2004), 24-34 (2004).
3. Hadjiargyrou, M., O'Keefe, R. J. The convergence of fracture repair and stem cells: interplay of genes, aging, environmental factors and disease. *Journal of Bone and Mineral Research.* **29** (11), 2307-2322 (2014).
4. De Becker, A., Riet, I. V. Homing and migration of mesenchymal stromal cells: How to improve the efficacy of cell therapy? *World Journal of Stem Cells.* **8** (3), 73-87 (2016).
5. Chen, Y., Song, S., Yan, Z., Fenniri, H., Webster, T. J. Self-assembled rosette nanotubes encapsulate and slowly release dexamethasone. *International Journal of Nanomedicine.* **6**, 1035-1044 (2011).
6. Song, S., Chen, Y., Yan, Z., Fenniri, H., Webster, T. J. Self-assembled rosette nanotubes for incorporating hydrophobic drugs in physiological environments. *International Journal of Nanomedicine.* **6**, 101-107 (2011).
7. Fenniri, H. et al. Helical Rosette Nanotubes: Design, Self-Assembly, and Characterization. *Journal of the American Chemical Society.* **123** (16), 3854-3855 (2001).
8. Chen, Y. et al. Self-assembled rosette nanotube/hydrogel composites for cartilage tissue engineering. *Tissue Engineering Part C Methods.* **16** (6), 1233-1243 (2010).
9. Van den Bogaerdt, A. J. et al. Collagen cross-linking by adipose-derived mesenchymal stromal cells and scar-derived mesenchymal cells: Are mesenchymal stromal cells involved in scar formation? *Wound Repair and Regeneration.* **17** (4), 548-558 (2009).
10. Erickson, H. P., Carrell, N., McDonagh, J. Fibronectin molecule visualized in electron microscopy: a long, thin, flexible strand. *Journal of Cell Biology.* **91** (3), 673-678 (1981).
11. Chen, Q., Yu, H.C., Chen, Y.P. *Patent US20170362238A1.* (2017).
12. Zhou, L. et al. Self-assembled biomimetic Nano-Matrix for stem cell Anchorage. *Journal of Biomedical Materials and Research.* **108**, 984-991 (2020).
13. Jones, M., Leroux, J., Polymeric micelles - a new generation of colloidal drug carriers. *European Journal of Pharmaceutics and Biopharmaceutics.* **48** (2), 101-111 (1999).
14. Singh, P., Schwarzbauer, J. E. Fibronectin and stem cell differentiation - lessons from chondrogenesis. *Journal of Cell Science.* **125**, 3703-3712 (2012).
15. Martino, M. M. et al. Controlling integrin specificity and stem cell differentiation in 2D and 3D environments through regulation of fibronectin domain stability. *Biomaterials.* **30** (6), 1089-1097 (2009).
16. Somaiah, C. et al. Collagen promotes higher adhesion, survival and proliferation of mesenchymal stem cells. *PLoS One.* **10** (12), e0145068 (2015).
17. Ogura, N. et al. Differentiation of the human mesenchymal stem cells derived from bone marrow and enhancement of cell attachment by fibronectin. *Journal of Oral Science.* **46** (4), 207-213 (2004).
18. Do, A. V., Khorsand, B., Geary, S. M., Salem, A. K. 3D Printing of scaffolds for tissue regeneration applications. *Advanced Healthcare Materials.* **4** (12), 1742-1762 (2015).
19. Shi, W. et al. Structurally and functionally optimized silk-fibroin-gelatin scaffold using 3D printing to repair cartilage injury in vitro and in vivo. *Advanced Material.* **29**, 1701089 (2017).
20. Journeay, W. S., Suri, S. S., Moralez, J. G., Fenniri, H., Singh, B. Low inflammatory activation by self-assembling Rosette nanotubes in human Calu-3 pulmonary epithelial cells. *Small.* **4** (6), 817-823 (2008).
21. Journeay, W. S., Suri, S. S., Moralez, J. G., Fenniri, H., Singh, B. Rosette nanotubes show low acute pulmonary toxicity in vivo. *International Journal of Nanomedicine.* 3 (3), 373-383 (2008).

